Supporting information:

Journal: Journal of Materials Chemistry A

Title:

New Generation Perovskite Solar Cells with Solution-Processed Amino-substituted Perylene Diimide Derivative as Electron-Transport Layer

Hua Zhang,[a, ‡] *Lingwei Xue,* [b, ‡] *Junbo Han,*[c] *Yong Qing Fu,* [d] *Yan Shen,* [a] *Zhiguo Zhang,* [b*] *Yongfang Li,* [b] *Mingkui Wang* [a*]

[a] Michael Grätzel Center for Mesoscopic Solar Cells, Wuhan National Laboratory for Optoelectronics, Huazhong University of Science and Technology, Luoyu Road 1037, Wuhan, 430074, P. R. China
[b] CAS Key Laboratory of Organic Solids, Institute of Chemistry, Chinese Academy of Sciences, Beijing 100190, China
[c] Wuhan National High Magnetic Field Center, Huazhong University of Science and Technology, 1037 Luoyu Road, Wuhan 430074, China
[d] Department of Physics and Electrical Engineering, Faculty of Engineering and Environment, Northumbria University, Newcastle Upon Tyne, NE1 8ST, UK

‡These authors contributed equally.
E-mail: mingkui.wang@mail.hust.edu.cn
E-mail: zgzhangwhu@iccas.ac.cn

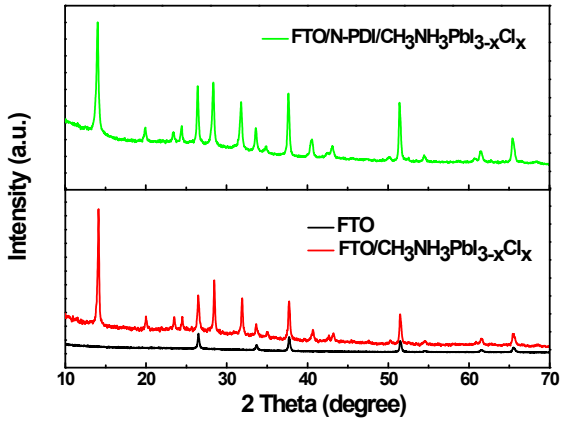

Figure S1 XRD pattern of $MAPbI_{3-x}Cl_x$ thin film on FTO and FTO/N-PDI. There is no distinct peaks at 2θ = 12.56 º, corresponding to the absence of typical diffractions of (001) planes for the unconverted PbI_2.

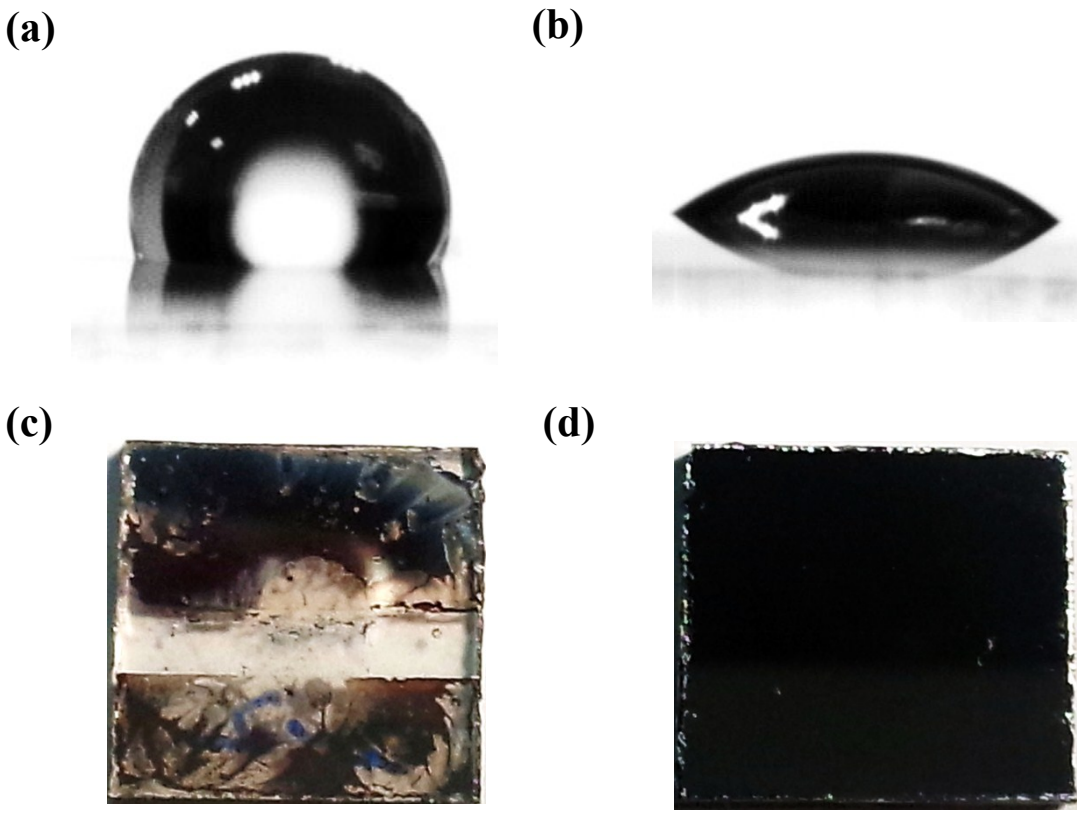

Figure S2. The contact angle of water on (a) FTO/C-PDI substrate, and (b) FTO/N-PDI substrate. Photograph of $MAPbI_{3-x}Cl_x$ film on (c) FTO/C-PDI and (d) FTO/N-PDI substrates, respectively.

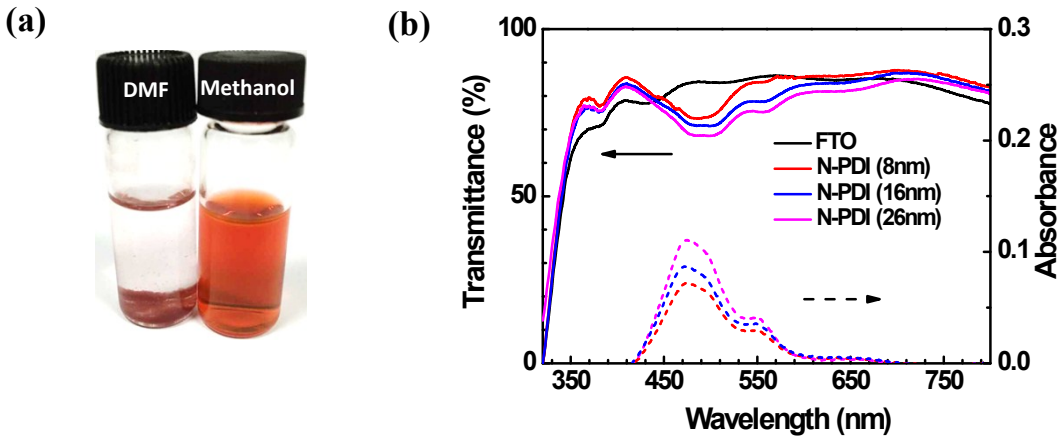

Figure S3. (a) Photograph of N-PDI in N, N-Dimethyl-formamide and methanol, showing the solubility of this material in different solvents. (b) Absorption (right ordinate) and transmittance (left ordinate) spectra of the FTO deposited with N-PDI interlayer by varying the thickness.

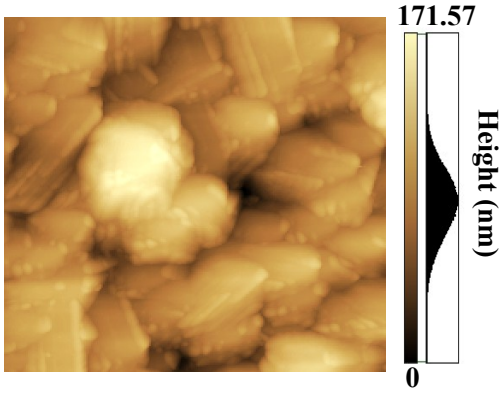

Figure S4. AFM image (size: 2×2 μm) of the FTO substrate, showing a roughness of 17.16 nm.

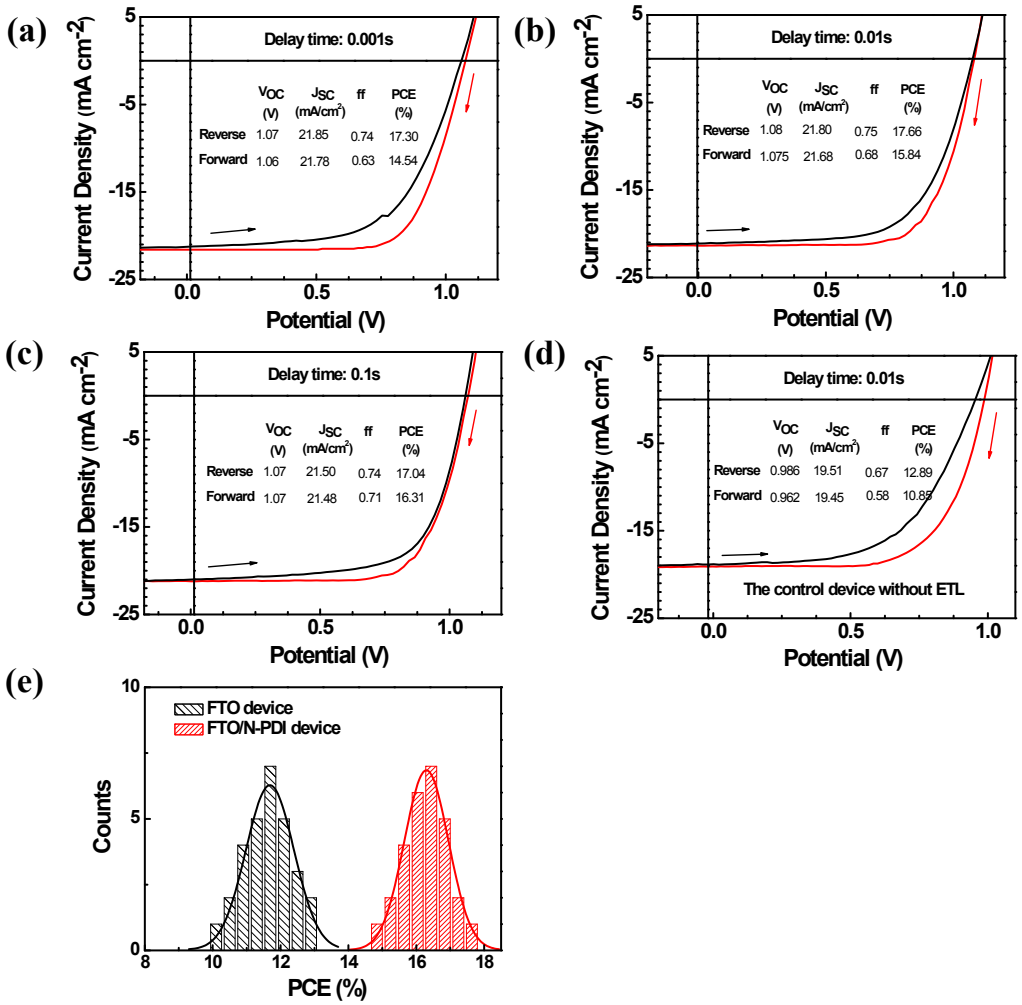

Figure S5. (a-c) Influence of scan rates on the current-voltage characteristics for the device based on FTO/N-PDI substrate (d) Current–voltage curves for the control device measured by forward and reverse scans at 20 mV per step with a delay time of 10 ms (e) Histogram of PCE for perovskite solar cells based on the FTO and FTO/N-PDI substrates.

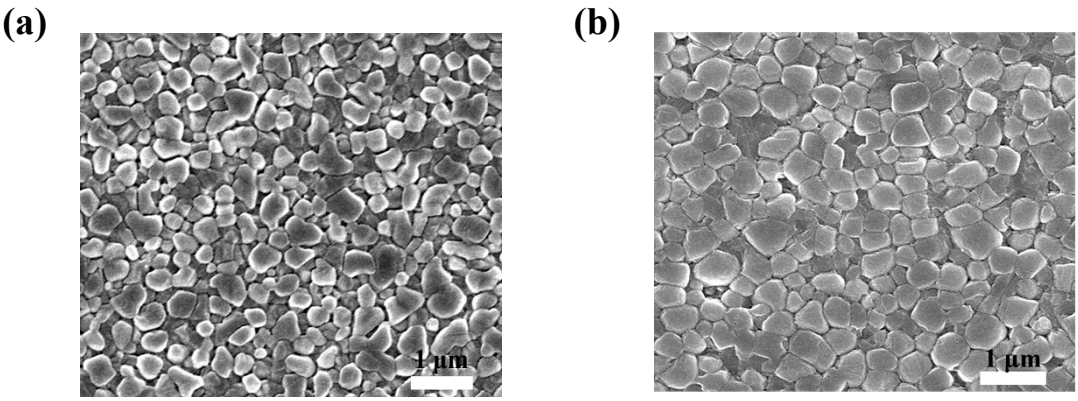

Figure S6 Top-view SEM images of the $MAPbI_{3-x}Cl_x$ films on (a) the FTO, and (b) the FTO/N-PDI substrates.

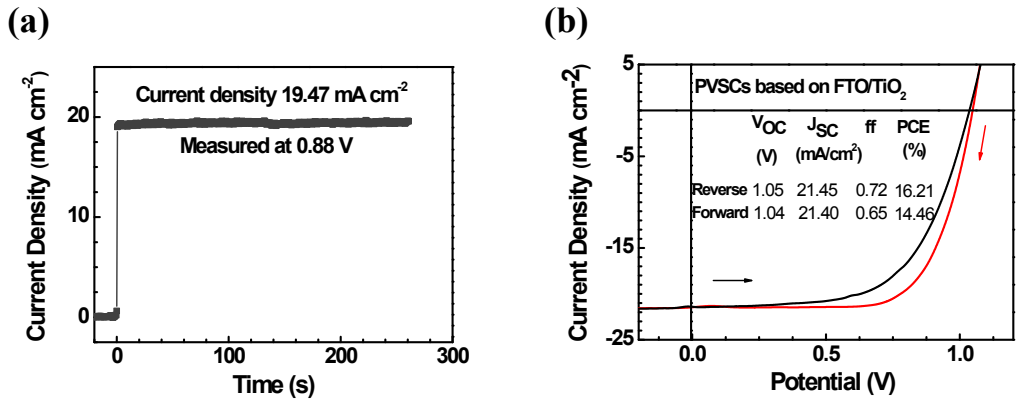

Figure S7 (a) Steady-state photocurrent output at the maximum power point (0.88 V) for the N-PDI based devices (b) J-V curves of the perovskite solar cells based on FTO/TiO_2 with different scan directions.

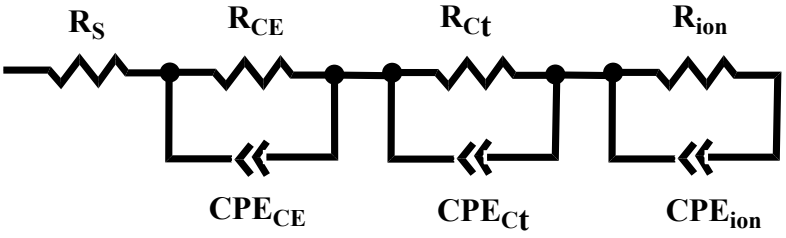

Figure S8 The equivalent circuit with 3 lumped RC-circuits in series for fitting the impedance spectroscopy data obtained from the perovskite solar cells in this study.

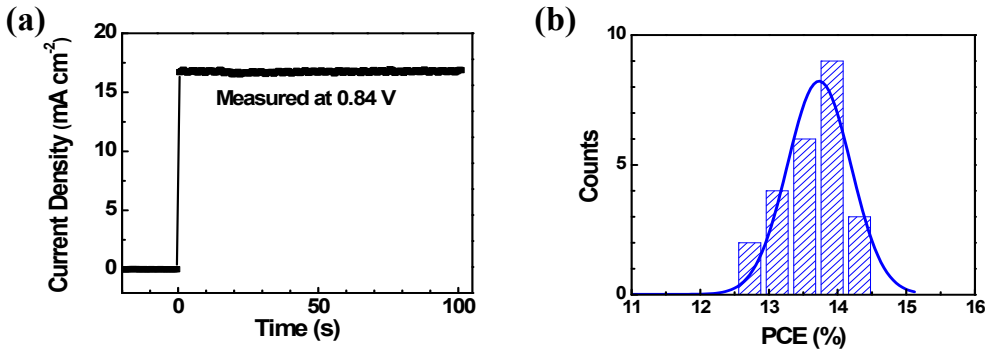

Figure S9 (a) Steady-state photocurrent output at the maximum power point (0.84 V) for the flexible perovskite solar cells based on N-PDI (b) Histogram of PCE for the flexible devices based on N-PDI.

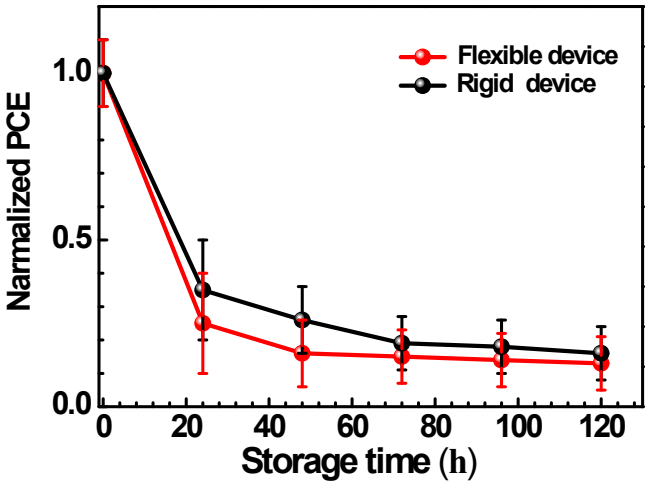

Figure S10 Normalized cell efficiency plotted as a function of storage time for the PVSCs based on rigid and flexible substrates, the devices without encapsulation were stored under ambient conditions (relative humidity ca. 50%; temperature ca. 28 ºC).